Simulating preferential soil water flow and tracer transport using the Lagrangian Soil Water and Solute Transport Model

Alexander Sternagel[1,2], Ralf Loritz[1], Wolfgang Wilcke[2], Erwin Zehe[1]

5 [1] Karlsruhe Institute of Technology (KIT), Institute of Water Resources and River Basin Management, Chair of Hydrology
[2] Karlsruhe Institute of Technology (KIT), Institute of Geography and Geoecology, Geomorphology and Soil Science

Correspondence to: Alexander Sternagel (alexander.sternagel@kit.edu)

Abstract. We propose an alternative model to overcome the weaknesses of the Darcy-Richards approach and to simulate preferential soil water flow and tracer transport in macroporous soils. Our LAST-Model (**La**grangian

10 Soil Water and **S**olute **T**ransport) relies on the movement of water particles carrying a solute mass through the soil matrix and macropores. We advance the model of Zehe and Jackisch (2016) by two main extensions: a) a new routine for solute transport within the soil matrix and b) the implementation of an additional 1-D preferential flow domain which simulates flow and transport in a population of macropores. Infiltration into the matrix and the macropores depends on their moisture state and subsequently macropores are gradually filled.

15 Macropores and matrix interact through diffusive mixing of water and solutes between the two domains which depends on their water content and matric potential at the considered depths.

The LAST-Model is evaluated by sensitivity analyses and tested against data of tracer field experiments at three different sites. The results corroborate the feasibility of the model approach and its ability to simulate preferential flow through macropores in a good accordance with observed tracer data. Yet, the model operates at

20 a high computational efficiency resulting in short simulation times and it provides a promising framework to improve the linkage between field experiments and computer models to reduce working effort, as well as to improve the understanding of preferential flow processes.

1 Introduction

Until now, the most common used hydrological models have been following an Eulerian perspective on the flow

25 processes with a stationary observer balancing dynamic changes in a control volume. The alternative Lagrangian perspective with a mobile observer travelling along the trajectory of a solute particle through the system (Currie, 2002) has up to now only been used to simulate advective-dispersive transport of solutes (Delay und Bodin, 2001; Zehe et al., 2001; Berkowitz et al., 2006; Koutsoyiannis, 2010; Klaus and Zehe, 2011). However, this particle tracking approach is mostly embedded in frameworks with Eulerian control volumes which still

30 characterize the dynamics of the carrying fluid. Lagrangian descriptions of the fluid dynamics itself are only realized in a few models. But such a particle tracking framework may offer many advantages, especially at the coping of the challenges induced by preferential water flow and solute transport in structured heterogeneous soils.

Preferential flow has become an major issue in hydrological research since the benchmark papers of Beven and

35 Germann (1982); Flury et al. (1994) and Uhlenbrook (2006). The term of preferential flow is used to summarize a variety of mechanisms leading to a rapid water movement in soils. The most prominent one is the flow through

non-capillary macropores (Beven and Germann, 2013) where water and solutes travel in a largely unimpeded manner due to the absence of capillary forces and bypass the soil matrix (Jarvis, 2007). Macropores can be classified into earth worm burrows, channels from degraded plant roots or shrinkage cracks and all of them are not static in space nor time (e.g. Blouin et al., 2013; Nadezhdina et al., 2010; Palm et al., 2012; van Schaik et al.,

5   2014; Schneider et al., 2018). Especially in rural areas and in combination with agrochemicals macropore flow can be a dominant control on stream and groundwater pollution (e.g. Flury, 1996; Arias-Estévez et al., 2008). To understand such water and solute movements a combination of plot scale experiments and computer models is commonly used (Zehe et al., 2001; Šimůnek and van Genuchten, 2008; Radcliffe and Šimůnek, 2010; Klaus and Zehe, 2011). One of the most frequently used approaches to simulate water flow dynamics and solute transport is

10   to use the Darcy-Richards and the advection-dispersion equation. Both equations fundamentally assume that solute transport is controlled by the interplay of advection and dispersion (Roth, 2006; Beven and Germann, 2013) and that the underlying soil water dynamics are dominated by capillary driven diffusive flow. While the second assumption is well justified in homogeneous soils, it frequently fails in soils with macropores. Consequently, we separate at least two flow regimes in soils: the slow diffusive flow in the soil matrix and the

15   rapid advective flow in the macropores. Partial mixing between these two flow regimes is non-trivial as it depends on the hydraulic properties of the macropore walls, the water content of the surrounding soil, actual flow velocities, hydrophobicity of organic coatings and much more. The inability of the Richards equation to simulate partial mixing between both flow regimes is well known and a variety of different models have been proposed to address this problem (Šimůnek et al., 2003; Beven and Germann, 2013). But most of them are

20   fundamentally still based on the Darcy-Richards equation like the most prominent and well-established double-domain models.

A promising alternative approach is provided by particle-based Lagrangian models for subsurface fluid dynamics. The first implementation of such a model for soil water dynamics is the SAMP model proposed by Ewen (1996a; b). SAMP represents soil water by a large number of particles travelling in an one-dimensional

25   soil domain by means of a random walk which is based on soil physics and soil water characteristics. A more recent example is the two-dimensional MIP model of Davies et al. (2013) developed for hillslopes. Fluid particles travel according to a distribution function of flow velocities which needs to be estimated from tracer field experiments. Exchange of particles among the different pathways is conceptualized as random process following an exponential distribution of mixing times. Inspired by the SAMP model, Zehe and Jackisch (2016)

30   conceptualized a Lagrangian model describing soil water flow by means of a non-linear space domain random walk. In line with Ewen (1996), they estimated the diffusivity and the gravity driven drift term of the random walk based on the soil water retention curve ($\Psi(\theta)$) and the soil hydraulic conductivity curve ($k(\theta)$).

The particle-based Lagrangian model of Zehe and Jackisch (2016) initially assumed that all particles travel at the same diffusivity and velocity corresponding to the actual soil water content. But a comparison to a Richards

35   solver revealed that this straightforward, naive random walk implementation highly overestimates infiltration and redistribution of water in the soil. The solution for this overestimation was to account for variable diffusive velocities. Now, particles in different pore sizes travel with various diffusivities, which are determined based on the shape of the soil hydraulic conductivity curve. This approach reflects the idea that the actual soil water content is the sum of volume fractions that are stored in different pore sizes and that the different pore sizes

40   constitute flow paths which differ in both advective and diffusive velocities.

Recently, this model was advanced by Jackisch and Zehe (2018) with the implementation of a second dimension which contains spatially explicit macropores to simulate preferential flow. Within a macropore the velocity of each particle is described by interactions of driving and hindering forces. Driver is the potential energy of a particle while energy dissipation due to friction at the macropore walls dissipates kinetic energy and accordingly

5 reduces particle velocities. With this approach, Jackisch and Zehe (2018) tried to make maximum use of observables for model parametrisation. The assets of their echoRD model are a self-controlling macropore film flow and its ability to represent 2-D infiltration patterns. The drawback of echoRD is the huge computational expense. The simulation time is about 10 to 200 times longer than real-time.

The huge computational expense of the echoRD model is one main motivation for us to develop a Lagrangian

10 approach which balances necessary complexity with greatest possible simplicity. The other motivation is the inability of all models mentioned above to simulate solute transport appropriately. This is essential for a rigorous comparison of the model with tracer data and to get closer to the simulation of reactive transport. Thus, the main objectives of this study are to:

1) Present a new routine for solute transport and diffusive mixing for well-mixed matrix flow conditions
15   which is implemented into the model of Zehe and Jackisch (2016) and to test this approach against tracer data from plot-scale experiments carried out in the Weiherbach catchment (Zehe and Flühler, 2001b).

2) Extend the model by implementing a macropore domain accounting for preferential flow of water and solutes and related exchange with the matrix domain. In contrast to the echorRD model, we maintain
20   the one-dimensional approach to keep the computational expense moderate.

The structure of our LAST-Model (**La**grangian **S**oil Water and **S**olute **T**ransport) is hence similar to a double-domain approach. The main asset is that flow and transport in both domains and their exchange are described by the same stochastic physics. This fact may help to overcome the limiting assumptions of the Darcy-Richards and

25 the advection-dispersion equation. The refined LAST-Model is tested with extensive sensitivity analyses to corroborate its physical validity. Further, it is also verified with a tracer experiment at a site in the Weiherbach catchment that is clearly dominated by preferential flow in macropores.

2 Concept and implementation of the LAST-Model

2.1 The Lagrangian model of Zehe and Jackisch (2016) in a nutshell

30 The basis of our development is the Lagrangian model of Zehe and Jackisch (2016). It describes infiltration and water movement through a spatial explicit 1-D soil domain dependent on the effects of gravity and capillarity in combination with a spatial random walk concept. Water is represented by particles with constant mass and volume. The density of soil water particles in a grid element represents the actual soil water content $\theta(t)$ [m³/m³] which reflects in turn the sum of the volume fractions of soil water that are stored in pores of strongly different

35 sizes. Water particles travel at different velocities in these pores which are characterized by the shape of the hydraulic conductivity and water diffusivity curve. The curves are subdivided into N bins, starting from the residual moisture θ_r stepwise to the actual moisture $\theta(t)$ using a step size of $\Delta\theta = \frac{(\theta(t)-\theta_r)}{N}$ (Figure 1). The particle displacement within the bins is described by Equation 1:

$$z_i(t + \Delta t) = -\left(\frac{k(\theta_r + i \cdot \Delta \theta)}{\theta(t)} + \frac{\partial D(\theta_r + i \cdot \Delta \theta)}{\partial z}\right) \cdot \Delta t + Z\sqrt{2 \cdot D(\theta_r + i \cdot \Delta \theta) \cdot \Delta t} \qquad i = 1, \dots, N \qquad (1)$$

Where z is the vertical position [m], k the hydraulic conductivity [m/s], i the number of bins, D the water
5   diffusivity [m²/s], i.e. the product of the hydraulic conductivity $k(\theta)$ and the slope of the soil water retention
curve, t the simulation time [s] and Z a random, uniformly distributed number. The equation comprises two
terms. The first one represents gravity driven downward advection of each particle based on the hydraulic
conductivity, the second one is the diffusive term driven by capillarity. According to Figure 1 and Equation 1
particles in coarse pores travel more rapidly at a higher hydraulic conductivity due to wet conditions. In smaller
10   pores or during drier conditions the flow velocities are so small that the particles are in fact immobile. This
binning of particle velocities and diffusivities also opens the opportunity to simulate rainfall infiltration under
non-equilibrium conditions. To this end, infiltrating rainfall-event water is treated as second type of particles
which initially travel at gravity driven, rapid velocities in the largest pore fraction and experience a slow
diffusive mixing with the pre-event water particles of the matrix within a characteristic mixing time. Test
15   simulations revealed the Lagrangian model can simulate water dynamics under equilibrium conditions in good
accordance with a Darcy-Richards approach for three different soils. For a detailed description of the underlying
model concept and the derivation of the equations see the study of Zehe and Jackisch (2016).

2.2 Representation of solute transport in the LAST-Model

In a first step we implement a routine for solute transport into the particle model by assigning a solute
20   concentration C [kg/m³] to each particle. This implies that a particle carries a solute mass which is equal to its
concentration times its water mass. Due to the particle movements through the matrix domain the dissolved mass
experiences advective transport in every time step. Diffusive mixing among all particles is calculated after each
displacement step by summing up the entire solute mass in a grid element and dividing it by the mass of all
present water particles. The underlying assumption of perfect mixing among all particles in a grid element
25   requires a diffusive mixing time corresponding to the molecular diffusion coefficient and which is smaller than
the time step Δt, which is ensured by a sufficiently fine grid.

2.3 The macropore domain and representation of preferential flow

The second and main model extension is the implementation of a 1-D preferential flow domain considering the
influence of macropores on water and solute dynamics. This requires four main steps:
30   1.   Design of a physically based structure of the macropore domain;
2.   Conceptualisation of the infiltration process into the domains;
3.   Description of macropore flow and storage of water and solutes;
4.   Conceptualisation of diffusive mixing of particles between the macropore and the matrix domain.

2.3.1 The preferential flow domain

35   We define a 1-D macropore or preferential flow domain (pfd) which is surrounded by a 1-D soil matrix domain
with vertically distinct boundaries. In line with other Lagrangian models, we represent water as particles with

constant mass and volume corresponding to their domain affiliation. As the vertical extent and volume of the pfd is much smaller than that of the matrix domain the corresponding particles must be much smaller to ensure that an adequate number of particles travel within the pfd for a valid stochastic approach.

The pfd comprises a certain amount of macropores. Each macropore has the shape and structure of a straight
5   circular cylinder with a predefined length and diameter containing spherically shaped particles (Figure 2a). Two of the most important geometry properties of the pfd are the macropore diameter $dmac$ (m) and the total number of macropores $nmac$ (-) as they scale exchange fluxes and determine several other characteristics like the total macropore volume. The hydraulic conductivity of the pfd k_{pfd} [m/s] and the advective velocity of a particle within the pfd v [m/s] are equal and dependent on the diameter as described in section 2.4.2. All other important
10   pfd parameters are defined in Figure 2.

Our 1-D approach can of course not account for the lateral positions of the macropores but the pfd allows a depth distribution of macropores which is important for calculating the depth-dependent exchange with the matrix (section 2.3.4). To calculate the water content and tracer concentrations, the pfd is vertically subdivided into grid elements. Therefore, water contents and solute concentrations are regarded as averaged over these grid elements.
15   Within a grid element of the pfd we assume cubic storage of particles (c.f. Figure 2a). The concept of cubic storage facilitates the calculation of the proportion of particles having contact to the lateral surface of a grid element. This proportion of the total amount of particles roughly corresponds to the hydraulic radius scaling the wetted cross section with the wetted contacted area in a macropore. Within the mixing process only the contact particles are able to infiltrate via the interface into the soil matrix.

20   **2.3.2 Infiltration and partitioning of water into the two domains**

As a 1-D approach does not allow an explicit, spatial distribution of the incoming precipitation water over the soil surface, we use an implicit, effective infiltration concept. The infiltration and distribution of water are controlled by the actual soil moisture and the flux densities driven by the hydraulic conductivity and the hydraulic potential gradient of the soil matrix as well as by friction and gravity within the macropores (Weiler,
25   2005; Nimmo, 2016). For example, a soil matrix with a low hydraulic conductivity increases the proportion of water infiltrating the macropores as it preferentially uses pathways of low flow resistance.

In our model, incoming precipitation water accumulates in a fictive surface storage from which infiltration water masses and related particle numbers are calculated. To this end, we distinguish several cases. In Case 1 the top soil grid elements of the soil matrix and the pfd are initially unsaturated and the infiltration capacity of the soil
30   matrix is smaller than the incoming precipitation flux density. Water infiltrates the soil matrix and the excess water is redistributed to the pfd and infiltrates it with a macropore-specific infiltration capacity. Case 2 applies when the top matrix grid element is saturated and water exclusively infiltrates the pfd until all macropores are also saturated. Case 3 occurs when both the top matrix layer and the pfd are saturated leading to an accumulation of precipitation water in the surface storage. As soon as the water contents in the first soil matrix grid element
35   and in the pfd are subsequently decreasing due to downward water flow or drainage of the macropores, again infiltration occurs according to Case 1. The incoming precipitation mass (m_{rain}) and the infiltrating water masses into the matrix (m_{matrix}) and the pfd (m_{pfd}) are calculated with Equations 2-4:

$$m_{rain} = q_{rain} * \rho_w * dt * A \tag{2}$$

$$m_{matrix} = \left(\frac{k\_m_1 + k_S}{2}\right) * \left(\frac{\psi_1 - \psi_2}{dz} + 1\right) * A * \rho_w * dt \tag{3}$$

$$m_{pfd} = k_{pfd} * \pi * \left(\frac{D_M^2}{2}\right) * \rho_w * dt * n_{mac} \tag{4}$$

Where q_{rain} [m/s] is the precipitation flux density respectively the intensity, k_m1 [m/s] the actual hydraulic

5   conductivity of the first grid element of the matrix, k_s [m/s] the saturated hydraulic conductivity of the matrix
and $\psi_1 - \psi_2$ [m] the matric potential gradient between the first two grid elements, k_{pfd} [m/s] the saturated
hydraulic conductivity of a macropore (c.f. section 2.4.2), D_M [m] the diameter of a macropore and n_{mac} the total
amount of macropores within the pfd, ρ_w [kg/m³] the water density, dt [s] the simulation time step and A [m²] the
plot area.

10   After the precipitation water has infiltrated into the two domains the masses are converted to particles which are
initially stored in the first grid elements of the matrix and pfd. They are now ready for the displacement process.

2.3.3 Advective flow in the macropores

In the pfd we assume a steady state balance between gravity and dissipative energy loss at the macropore walls.
This implies purely advective flow characterised by a flow velocity v which can either be inferred from tracer or
15   infiltration experiments on macroporous soils as described by Shipitalo and Butt (1999); Weiler (2001) and Zehe
and Blöschl (2004). The particle displacement in our pfd is described by Equation 5:

$$\Delta z = v \cdot \Delta t \tag{5}$$

20   As all particles in the pfd travel at the same velocity their displacement depends on the time step. Because
Lagrangian approaches are not subject to time step restrictions we are free to scale the time step in such a way
that a displacement step Δz of a particle entering the pfd corresponds to the deepest unsaturated grid element of
the pfd. The underlying particle displacement concept (Figure 2b) is comparable to the filling of a bottle with
water. Water initially flows to the bottom of the empty macropore and in the following it is gradually filled up to
25   the top. This simple volume filling method was applied before in other models, e.g. in the SWAP model of van
Dam et al. (2008) or in the study of Beven and Clarke (1986). If a grid element gets oversaturated in this way,
the excess water particles will be stored in the next unsaturated grid element above. In line with the matrix,
particle densities are calculated in each grid element to obtain the actual soil water content and tracer
concentrations of the pfd.

30   ### 2.3.4 Water and tracer exchange between the macropore and the matrix domain

Commonly, macropore-matrix interactions are challenging to observe within field experiments. One approach is
to evaluate isotopic composition of water in the two domains (Klaus et al., 2013). In theory it is often assumed
that the interactions and water dynamics at the interface between macropores and the matrix are mainly
controlled by the matric head gradients and the hydraulic conductivity of both domains which depend on an
35   exchange length and the respective flow velocities (Seven and Germann, 1981; Gerke, 2006).

Our model approach is also based on these assumptions as illustrated in Figure 2c. We restrict exchange to the saturated parts of the pfd assuming downward particle transport as being much larger than the lateral exchange and we neglect diffusive exchange between solutes in the matrix and the pfd. We are aware that these simplifications might constrain the generality of our model. For instance, we also neglect the effect of a reverse

5   diffusion from the matrix into the macropores. This effect can influence water and solute dynamics when the propagation of a pressure wave pushes matrix water into empty macropores, mainly in deeper saturated matrix areas (Beven and Germann, 2013). We rely on those simplifications a) to keep the model simple and efficient and b) because the focus of our model is on unsaturated soil domains and during rainfall driven conditions the macropores are completely filled due to their small storage volume most of the time.

10   Generally, our model divides the total amount of macropores n_{mac} within the pfd into three depths. For that reason, the total number is multiplied with a distribution factor f for big (f_{big}), medium (f_{med}) and small (f_{sml}) macropores. The saturated grid elements (blue filled) of the largest macropores are coupled to the respective grid elements of the medium and small macropores. In this example, the red respectively the black framed grid elements of the three macropore sizes are coupled due to their saturation state and depth order. This coupling

15   ensures a simultaneous diffusive water flow out of the respective grid elements of all three macropore depths. The mixing fluxes (q_{mix} [m³/s]) in the actual grid elements are calculated by Equation 6:

$$q_{mix} = \frac{2 \cdot k_{pfd} \cdot k\_m_i}{(k_{pfd} + k\_m_i)} \cdot \frac{\psi_i}{D_M} \cdot C \cdot dz \qquad (6)$$

20   Thus, diffusive mixing fluxes are calculated with the harmonic mean of the saturated hydraulic conductivity of the pfd k_{pfd} [m/s] and the hydraulic conductivity of the respective matrix grid element k_m_i [m/s], multiplied with the relation of the matric potential ψ_i [m] of the actual matrix grid element and the grid element diameter D_M [m] as exchange length and the circumference C [m] of the macropore grid element.

The mixing masses are again converted into particle numbers with the two different particle masses. Due to the

25   higher masses of the matrix particles a much lower amount of particles is entering the matrix. This has to be taken into account by choosing an adequate number of total particles present within the matrix, i.e. at least one million at high saturated hydraulic conductivities. In addition, it is ensured the number of particles leaving a grid element of the pfd is lower than the maximum possible number of particles having contact to the lateral surface (cf. section 2.3.1) dependent on its actual soil water content. Furthermore, the model routine gives the

30   opportunity to activate an additional diffusive drainage with particles leaving the macropores at their lower boundary.

2.4 Model setup

2.4.1 Evaluation of the solute transport and linear mixing approach during well-mixed matrix flow

Basis of the first evaluation of our solute transport and linear mixing approach are data from tracer experiments

35   conducted by Zehe and Flühler (2001b) in the Weiherbach catchment to investigate mechanisms controlling flow patterns and solute transport. The Weiherbach-valley is located in the southwest of Germany and has a total extent of 6.3 km². Basic geological formations comprise Keuper and Loess layers with a thickness of up to 15 m.

The hillslopes exhibit a typical Loess catena with Colluvisols at the foot and Calcaric Regosols or Luvisols at the top and mid slopes. Landuse is highly dominated by agriculture.

Within this catchment, a series of irrigation experiments with bromide as tracer were performed at ten sites. At each site a plot area of 1.4 m x 1.4 m was defined and the initial soil water content and the soil hydraulic

5   functions were measured. The plot area was then irrigated by a block rainfall of approx. 10 mm/h with a tracer solution containing 0.165 g/l bromide. After one day soil profiles were excavated and soil samples were collected in a 0.1 m x 0.1 m grid and their corresponding bromide concentrations measured. More details on the tracer experiments can be taken from Zehe and Flühler (2001a; b). For the model evaluation, we select the two sites 23 and 31 where flow patterns reveal a dominance of well-mixed matrix flow. The present soil at the two

10   sites can be classified as Calcaric Regosol (Wrb, 2015). All experimental and model parameters as well as the soil properties at these sites are listed in

Table 1.

2.4.2 Evaluation of the preferential flow domain

In a next step, our pfd model extension is again evaluated with the help of the results of another field tracer experiment of Zehe and Flühler (2001b). This time we select the site Spechtacker which shows numerous worm

5   burrows inducing preferential flow. The site is also located in the Weiherbach catchment and the present soil can be classified as Colluvic Regosol (Wrb, 2015). The macropore system of the sampled plot was carefully examined by measuring of depths, diameters and area density of the macropores. Zehe and Blöschl (2004) measured water flow through a set of undisturbed soil samples containing macropores of different radii at this site. In line with the law of Hagen-Poiseuille, they found a strong proportionality of the flux through the

10 macropores to the square of the macropore radius while frictional losses where 500 to 1000 times larger. Based on these findings, the hydraulic conductivity of the macropores k_{pfd} was calculated as a function of the diameters or radii r_M (Equation 7).

$$k_{pfd} = 2884.2 \cdot r_M{}^2 \tag{7}$$

For more details of the site Spechtacker and its macropore network, see the studies of Ackermann (1998) and Zehe (1999). All experiment and simulation parameters, soil properties and information about the macropore network at the site Spechtacker are also listed in Table 1.

2.4.3 Sensitivity analyses of selected parameters

20 The sensitivity analyses of the model with the pfd-extension are conducted with Monte Carlo simulations by varying several parameters describing the soil matrix and the pfd in a realistic value range. To this end, the saturated hydraulic conductivity of the matrix k_s, the diameter *dmac* and the amount *nmac* of the macropores are the selected parameters which are deemed to be most sensitive and crucial for the model behaviour and the simulation results. Moreover, different configurations of the macropore depth distribution and the distribution

25 factors are evaluated. The depth distribution of macropores thereby comprises a deep (Configuration 1), medium (Configuration 2) and shallow (Configuration 3) distribution. At the distribution factors there are four different configurations. A realistic distribution comprising more small than big macropores is represented by Configuration 1 and 4, a homogenous distribution is shown by Configuration 2 and a rather uncommon distribution with more big than small macropores is illustrated by Configuration 3. All parameter ranges and the

30 detailed configurations of the sensitivity analyses are listed in Table 2.

The probably most sensitive parameter is k_s as it controls the infiltration capacities of both domains, the displacement within the soil matrix as well as the diffusive mixing fluxes. Beside the saturated hydraulic conductivity of the matrix, also the amount and geometry of the macropores are of great importance for the model results as described above in section 2.3.1. All model runs were performed at the site Spechtacker using

35 22 mm rainfall in 140 minutes with subsequent drainage duration of one day. Additional parameters like soil properties, antecedent moisture and concentration states, bromide concentration of precipitation water and distribution of macropores remain constant (c.f. Table 1).

3 Results

3.1 Simulation of solute transport under well-mixed conditions

Note that the corresponding observations provide the tracer concentration per dry mass of the soil C_{dry} while LAST simulates concentrations in the water phase C_w. We thus compare simulated and observed tracer mass in

5   the respective depths. The well-mixed sites 23 and 31 show a high similarity due to their spatial proximity (Figure 3a, b). The shape and courses of the simulated tracer mass profiles coincide well with the observed ones over the entire soil domain and the observed values are within the uncertainty range of the simulations, represented by the rose shaded areas. This area reflects the uncertainty arising from a variation of k_s values of the soil matrix in the observed range of 10^{-6} and 10^{-5} m/s.

10   Note that in the experiments the solute mass was not directly measured at the soil surface but the observations represent averages across 10 cm depth increments. A comparison of the simulated masses close to the surface is thus not meaningful. This difference between simulated and observed profiles near to the surface suggest that the coarse resolution of the sampling grid is a likely reason for the relatively low recovery rates of 77 % and 76 % at the two sites (c.f. Table 1). Overall, we conclude that manipulating k_s within the observed uncertainty leads to an

15   unbiased simulation ensemble compared to the observed tracer data at matrix flow dominated sites.

3.2 Evaluation of the preferential flow domain

Finally, our model with the new preferential flow domain is tested against a tracer experiment on a macroporous soil at the site Spechtacker. As the related uncertainty range is similar to sensitivity ranges presented in the previous section we do not show it here again. The simulated and observed tracer mass distributions are

20   generally in good accordance (Figure 3c). Especially in deeper soil regions from 0.35 m to 1 m the shape and the magnitude of values correspond well. In the upper soil parts from 0 m to 0.15 m the model slightly overestimates the solute masses. Between 0.15 m and 0.35 m soil depth both profiles exhibit the greatest differences and even contrary courses.

3.3 Sensitivity analyses

25   #### 3.3.1 Sensitivity to saturated hydraulic conductivity k_s

The concentration profile range of the matrix reveals a strong sensitivity of the simulated profiles to k_s when we neglect macropores (Figure 4a). Especially in the upper soil part the differences arising from low and high k_s values are clearly detectable. Lower values imply that the soil matrix has a smaller infiltration capacity and therefore less water is infiltrating the matrix. Consequently, without macropores solutes do not penetrate into

30   depths greater than 0.2 m. The presence of macropores significantly alters the sensitivity of the concentration and soil moisture profiles (Figure 4b, c). Again, the profile shapes clearly depend on the k_s values but now water and solutes reach greater depths of up to 0.8 m by flowing through the macropores. At low k_s values (red curve) the reduced matrix infiltration capacity leads to an increased infiltration of water and solute into the macropores. Subsequently, the solutes bypass the matrix until they diffusively mix into the matrix at greater depths.

35   In contrast, at high k_s values the matrix infiltration capacity is increased. This leads in turn to a reduced infiltration into the macropores and instead the majority of water and solute masses infiltrates the matrix and remains in the top soil. This effect is reflected by the blue curves in Figure 4 with higher solute concentrations

near the soil surface and decreased concentrations at greater depths in comparison to low k_s values. Figure 5 generally confirms these findings. The four temporal snapshots show the development of the concentration profiles at low, medium and high k_s values throughout the simulation time with a) + b) during the rainfall event and c) + d) shortly after it and after one day, respectively. It is obvious how rapidly solute concentrations

5 increase especially in the upper soil part at high k_s values. Shortly after the rainfall event almost the entire water and solute masses have infiltrated the matrix due to the higher infiltration capacity. At low k_s values water and solutes need notably more time to infiltrate completely. The differences of the centres of mass and the deeper shift of the mass centre at low k_s values confirm the increased macropore infiltration and penetration of solutes through them to greater depths.

10 Finally, the yellow curves in Figure 6 show the proportion of solutes within the matrix which originates from the macropores. In general, at all k_s values and depths below 0.2 m the entire solute amount within the matrix travelled through the macropores. Differences are restricted to the upper soil part. Here the largest proportion of solutes has directly infiltrated the matrix without having been in the macropores before. The pfd proportion decreases from low to high k_s values confirming again the important influence of the k_s values on the infiltration

15 capacities and the distribution of water and solutes.

3.3.2 Sensitivity to macropore amount *nmac* and diameter *dmac*

The model results sensitively respond to a variation of macropore diameters. In the upper soil part the solute concentrations and moisture are slightly higher, when macropores are small (Figures 7a, b). In this case, the macropores collect only smaller amounts of water and solutes and the majority has directly infiltrated the soil

20 matrix. Wider macropores transport larger amounts of water and solutes to greater depths where they diffusively mix into the subsoil matrix. This deep redistribution is reflected by the characteristic profile shapes and the higher concentration and moisture values in the deep soil. The development of the concentrations is similar for all macropore diameters with just marginal differences arising shortly after the rainfall event (Figure 8). While the macropore diameter has a minor influence in the initial phase, stronger differences occur at the end of the

25 simulation when the residual water and solute amounts of the fictive surface storage have finally infiltrated. The centres of mass corroborate the results of Figure 7 in the way that the big macropores have the tendency to transport more solute masses into the subsoil.

Furthermore, the influence of different macropore numbers on the concentration and moisture profiles is marginal (Figure 7c, d). This implies that the model do not respond to every geometry parameter equally

30 sensitively. The macropore amount scales less than the diameter at the calculation of the further macropore measures. However, this could change when working with higher precipitation intensities.

Simulations with different macropore depth configurations again reveal a clear sensitivity of the model (Figures 9a, b). A steady decrease of the deep redistribution of the concentration and moisture values from the deep (Configuration 1) to the shallow depth configuration (Configuration 3) is obvious. Shallow macropores distribute

35 the total amount of water and solutes mainly in the upper soil part, while deep macropores relocate this distribution to greater depths of up to 1 m. The results of the distribution factor configurations again corroborate the previous findings (Figures 9c, d). Configuration 2 produces a homogeneous solute concentration profile from 0.2 m to the total depth. Both more realistic Configurations 1 and 4 comprise more small than big macropores. This increased number of small macropores ensures higher water and solute amounts in the first 0.5 m of the soil

matrix due to an enhanced mixing in this area. Finally, the rather uncommon Configuration 3 with more big than small macropores shows converse results. Solute concentrations and moisture contents are strongly increased at great depths from 0.7 m to 1 m because of increased diffusive mixing fluxes in these parts.

4 Discussion and Conclusions

5   We extend the Lagrangian model of Zehe and Jackisch (2016) with routines to consider transport and linear mixing of solutes within the soil matrix as well as preferential flow through macropores and related interactions with the soil matrix. The evaluation of the model with data of tracer field experiments and the sensitivity analyses reveal the feasibility and physical validity of the model structure as well as the robustness of the solute transport and linear mixing approach. The LAST-Model provides a promising framework to improve the linkage
10   between field experiments and computer models to reduce working effort, and to improve the understanding of preferential flow processes.

4.1 New routine for solute transport and diffusive mixing

The initially performed simulations of the mass profiles at the two well-mixed sites 23 and 31 support the validity of the straightforward assumptions of the underlying solute transport routine with its perfect mixing
15   approach (Figures 3a, b). In the presented version our mixing routine works with a short mixing time to ensure an instantaneous mixing between event and pre-event particles to account for the well-mixed conditions at the selected sites. However, the model allows to select longer mixing times or even a distribution of various mixing times to consider imperfect mixing among different flow paths.

The capability of predicting the solute dynamics is hence a big asset of our approach and it is a solid base to
20   realize the second model extension with the implementation of the preferential flow domain.

4.2 Model extension to account for preferential flow in macropores

The results of the evaluation of the pfd-extension show that our model is furthermore capable to simulate a tracer experiment on a macroporous soil and to depict well its observed 1-D solute mass profile (Figure 3c).

Especially the solute masses in the subsoil match well between simulated and observed data. This corroborates
25   our assumptions concerning the macropore structure and the approach to describe macropore-matrix exchange which proved to be feasible to predict solute distribution patterns due to preferential flow and related long transport lengths. In this context, we stress that the approach to simulate macropore-matrix exchange (c.f. Figure 2c) does not rely on an extra leakage parameter but follows the theory of deriving an effective conductance. Deviations from the observations occur during the simulation of the mass profile in upper soil parts. However,
30   these deviations are smaller than the uncertainty ranges revealed by the sensitivity analyses (Figures 4, 7). Note that the conversion of solute masses into an integer number of particles results in small errors, leading to a small amount of solutes not entering the system and remaining in the fictive surface storage. To mitigate this model effect, a high number of total particles present in the matrix is necessary, at least two million. Beside many displacement steps of each particle, the total number of particles is important to render the random walk
35   approach statistically valid (Uffink, 1990), although too high particle numbers will decrease the computational efficiency. Thus, we conclude that our extension of the Lagrangian particle model of Zehe and Jackisch (2016) is

a promising tool for a straightforward 1-D estimation of non-uniform solute and water dynamics in macroporous soils. However, before the suitability of our model approach to simulate preferential flow of non-interacting tracers is generalized, further field experiments on a variety of differently structured soils is necessary.

5   Some of our assumptions like the macropore geometry, the simple volume filling or the depth distribution of macropores were applied in a similar way in dual-porosity models before (Seven and Germann, 1981; Workman and Skaggs, 1990; van Dam et al., 2008). Thus, our model extension can be seen as an advancement of double-domain approaches by assuming simple volume filling for macropore flow and particle tracking for matrix flow instead of relying on the Darcy-Richards equation. With these results, our model is one of the first which proves

10   that simulations based on a Lagrangian perspective on both solute transport and dynamics of the carrying fluid itself are possible and well applicable. Also, the vertically distributed exchange seems feasible and the concept of cubic particle storage within the macropores (c.f. Figure 2a, section 2.3.1) is strongly motivated by the hydraulic radius and can thus be transferred to any kind of macropore geometry.

15   Another remarkable result is the high model sensitivity towards the saturated hydraulic conductivity k_s of the soil matrix (Figures 4-6). Especially its direct influence on the infiltration process is crucial. As k_s determines the initialisation, infiltration fluxes and the distribution of incoming precipitation masses to the two domains, it has a direct impact on the deep displacement of water and solutes and its temporal evolution (Figure 5). Therewith, our findings highlight the importance of infiltration processes on macroporous soils and the challenge to implement

20   them properly into models which have also been stressed by other studies (Beven and Germann, 1982; Weiler, 2005; Nimmo, 2016).
Our model shows the highest sensitivity to the presence of a population of macropores while differences in macropore properties comparatively have little impact. Generally, wider macropores collect and transport more water and solutes to greater depths than small ones (Figures 7a, b), but mainly at the end of simulations this

25   difference and the influence of the macropores on the infiltration and the macropore-matrix mixing processes are remarkable, because the storage volume of the preferential flow domain is small and hence it can only collect small amounts of water and solutes in relation to the matrix domain (Figure 8). Furthermore, high numbers of macropores do not necessarily result in a greater and deeper percolation of solutes (Figures 7c, d). Jackisch and Zehe (2018) also reported this aspect and explain it with the distribution of the irrigation supply to all

30   macropores and this supply can drop below the diffusive mixing fluxes from the macropores into the matrix. However, this implies that the number of macropores becomes more sensitive at much larger irrigation rates.
Where and to which extent water and solutes are diffusively mixed from the macropores into the matrix clearly depends on the depth distribution of the macropores and the distribution of the mixing masses among the various depths (Table2, Figure 9). This concept of the distribution of macropore depths and mixing masses is important

35   to meet the natural condition of a high spatial heterogeneity of the macropore network.

At the end, we overall conclude that the modified 1-D structure of our model is robust and provides a high computational efficiency with short simulation times. The evaluation of the preferential flow domain with the selected parametrisation (c.f. Table 1) only runs for about five minutes, which is a big advantage of our model.

40   Moreover, the efficiency allows for the implementation of further routines with yet still appropriate simulation

times. In this way, the model could prospectively consider retardation and adsorption effects as well as first-order reactions during the transport of non-conservative substances like pesticides. Until now, the solute movement of conservative tracers like bromide is only determined by the water flow without any consideration of molecular diffusion or particle interactions, although some evidence suggests a non-conservative behaviour of
5   bromide tracers under certain conditions (e.g. Whitmer et al., 2000; Dusek et al., 2015). In our case, we believe that the event scale and the short simulation times allow for the assumption of a conservative behaviour of bromide.

Moreover, the model can be extended to 2-D for simulations on hillslope or even catchment scales. In this regard, our model also offers the promising opportunity to quantify water ages and to evaluate travel and
10   residence times of water and solutes by a simple age tagging of particles. This can shed light on the chemical composition and generation of runoff fluxes as well as on the "Inverse Storage Effect". This effect describes a greater discharge fraction of recent event water at a high catchment water storage than at low storage. (Hrachowitz et al., 2013; Harman, 2015; Klaus et al., 2015; van der Velde et al., 2015; Sprenger et al., 2018).

15   *Data availability.* The hydrological model LAST, the tracer and soil data as well as all simulation results are available from the leading author on request.

Competing interests. The authors declare that they have no conflict of interest.

20   *Acknowledgements.* This research contributes to the Catchments As Organized Systems (CAOS) research group (FOR 1598) funded by the German Science Foundation (DFG).

The article processing charges for this open-access publication were covered by a Research Centre of the Helmholtz Association.

5 References

Ackermann, M.: Hydrogeologische Systemanalyse und Grundwasserhaushalt des Weiherbach-Einzugsgebietes, PhD thesis, Lehrstuhl für Angewandte Geologie der Universität Karlsruhe, 1998.

Arias-Estévez, M., López-Periago, E., Martínez-Carballo, E., Simal-Gándara, J., Mejuto, J.-C., García-Río, L.: The mobility and degradation of pesticides in soils and the pollution of groundwater resources, Agriculture, Ecosystems & Environment 123 (4), 247–260, https://doi.org/10.1016/j.agee.2007.07.011, 2008.

Berkowitz, B., Cortis, A., Dentz, M., and Scher, H.: Modeling non-Fickian transport in geological formations as a continuous time random walk, Rev. Geophys., 44, RG2003, https://doi.org/10.1029/2005RG000178, 2006.

Beven, K. and Germann, P.: Macropores and water flow in soils revisited, Water Resour. Res., 49, 3071–3092, https://doi.org/10.1002/wrcr.20156, 2013.

Beven, K.; Clarke, R. T.: On the variation of infiltration into a homogeneous soil matrix containing a population of macropores, Water Resour. Res. 22 (3), 383–388, https://doi.org/10.1029/WR022i003p00383,1986.

Blouin, M., Hodson, M. E., Delgado, E. A., Baker, G., Brussaard, L., Butt, K. R., Dai, J., Dendooven, L., Peres, G., Tondoh, J. E.,Cluzeau, D., and Brun, J. J.: A review of earthworm impact on soil function and ecosystem services, Eur. J. Soil Sci., 64, 161–182, https://doi.org/10.1111/ejss.12025, 2013.

Currie, I. G.: Fundamental mechanics of fluids, CRC press, 2002

Davies, J., Beven, K., Rodhe, A., Nyberg, L., and Bishop, K.: Integrated modeling of flow and residence times at the catchment scale with multiple interacting pathways, Water Resour. Res., 49, 4738–4750, https://doi.org/10.1002/wrcr.20377, 2013.

Delay, F. and Bodin, J.: Time domain random walk method to simulate transport by advection-dispersion and matrix diffusion in fracture networks, Geophys. Res. Lett., 28, 4051–4054, https://doi.org/10.1029/2001GL013698, 2001.

Dusek, J., Dohnal, M., Snehota, M., Sobotkova, M., Ray, C., Vogel, T.: Transport of bromide and pesticides through an undisturbed soil column. A modeling study with global optimization analysis. Journal of contaminant hydrology 175, 1–16, https://doi.org/10.1016/j.jconhyd.2015.02.002, 2015.

Ewen, J.: 'SAMP' model for water and solute movement in un-saturated porous media involving thermodynamic subsystems and moving packets: 1. Theory, J. Hydrol., 182, 175–194, https://doi.org/10.1016/0022-1694(95)02925-7, 1996a.

Ewen, J.: 'SAMP' model for water and solute movement in unsaturated porous media involving thermodynamic subsystems and moving packets: 2. Design and application, J. Hydrol., 182, 195–207, https://doi.org/10.1016/0022-1694(95)02926-5, 1996b.

Flury, M. (1996): Experimental evidence of transport of pesticides through field soils—a review, Journal of environmental quality 25 (1), 25–45, doi:10.2134/jeq1996.00472425002500010005x, 1996

Flury, M., Flühler, H., Jury, W. A., and Leuenberger, J.: Susceptibility of soils to preferential flow of water: A field study, Water Re-sour. Res., 30, 1945–1954, https://doi.org/10.1029/94WR00871,1994.

Gerke, H.H.: Preferential flow descriptions for structured soils, J.PlantNutr.SoilSci., 169, 382–400, https://doi.org/10.1002/jpln.200521955, 2006.

Harman, C. J.: Time-variable transit time distributions and transport. Theory and application to storage-dependent transport of chloride in a watershed, Water Resour. Res., 51, 1–30, doi:10.1002/2014WR015707, 2015.

Hrachowitz, M., Savenije, H., Bogaard, T. A., Tetzlaff, D., Soulsby, C.: What can flux tracking teach us about water age distribution patterns and their temporal dynamics?, Hydrol. Earth Syst. Sci., doi:10.5194/hess-17-533-2013, 2013.

Jackisch, C., Zehe, E.: Ecohydrological particle model based on representative domains, Hydrol. Earth Syst. Sci. 22 (7), 3639–3662, doi:10.5194/hess-22-3639-2018, 2018.

Jarvis, N. J.: A review of non-equilibrium water flow and solute transport in soil macropores: principles, controlling factors and consequences for water quality, Eur. J. Soil Sci., 58, 523–546, https://doi.org/10.1111/j.1365-2389.2007.00915.x, 2007.

Klaus, J., Elsner, M., Külls, C., and McDonnell, J. J.: Macropore flow of old water revisited: experimental insights from a tile-drained hillslope, Hydrol. Earth Syst. Sci., 17, 103–118, https://doi.org/10.5194/hess-17-103-2013, 2013.

Klaus, J., Chun, K. P., McGuire, K. J., McDonnell, J. J.: Temporal dynamics of catchment transit times from stable isotope data, Water Resour. Res. 51 (6), 4208–4223, doi:10.1002/2014WR016247, 2015

Klaus, J. and Zehe, E.: A novel explicit approach to model bromide and pesticide transport in connected soil structures, Hydrol. Earth Syst. Sci., 15, 2127–2144, https://doi.org/10.5194/hess-15-2127-2011, 2011.

Koutsoyiannis, D.: HESS Opinions "A random walk on water", Hydrol. Earth Syst. Sci., 14, 585–601, https://doi.org/10.5194/hess-14-585-2010, 2010.

Nadezhdina, N., David, T. S., David, J. S., Ferreira, M. I., Dohnal,M., Tesar, M., Gartner, K., Leitgeb, E., Nadezhdin, V., Cermak,J., Jimenez, M. S., and Morales, D.: Trees never rest: the multiple facets of hydraulic redistribution, Ecohydrology, 3, 431–444, https://doi.org/10.1002/eco.148, 2010.

Nimmo, J. R.: Quantitative Framework for Preferential Flow Initiation and Partitioning, Vadose Zone J., 15, 1–12, https://doi.org/10.2136/vzj2015.05.0079, 2016.

Palm, J., van Schaik, L., and Schröder, B.: Modelling distribution patterns of anecic, epigeic and endogeic earthworms at catchment-scale in agro-ecosystems, Pedobiologia, 56, 23–31, https://doi.org/10.1016/j.pedobi.2012.08.007, 2012.

Radcliffe, D. E., Šimůnek, J..: Soil physics with HYDRUS. Modeling and applications, CRC press, 2010.

Roth, K.: Soil physics, Lecture Notes, Institute of Environmental physics, University of Heidelberg, http://www.iup.uniheidelberg.de/institut/forschung/groups/ts/students, 2006

Schäfer, D.: Bodenhydraulische Eigenschaften eines Kleineinzugsgebietes. Vergleich und Bewertung unterschiedlicher Verfahren, PhD thesis, Inst. für Hydromechanik, Universität Karlsruhe, 1999.

Schneider, A.-K., Hohenbrink, T. L., Reck, A., Zangerlé, A., Schröder, B., Zehe, E., van Schaik, L.: Variability of earthworm-induced biopores and their hydrological effectiveness in space and time, Pedobiologia 71, 8–19, https://doi.org/10.1016/j.pedobi.2018.09.001, 2018

Seven, K., Germann, P.: Water flow in soil macropores II. A combined flow model, Journal of Soil Science 32 (1), 15–29, https://doi.org/10.1111/j.1365-2389.1981.tb01682.x, 1981.

Shipitalo, M. J. and Butt, K. R.: Occupancy and geometrical proper-ties of Lumbricus terrestris L. burrows affecting infiltration, Pedobiologia, 43, 782–794, 1999.

Šimůnek, J., Jarvis, N. J., Van Genuchten, M. T., and Gärdenäs, A.: Review and comparison of models for describing non-equilibrium and preferential flow and transport in the vadose zone, J. Hydrol., 272, 14–35, https://doi.org/10.1016/S0022-1694(02)00252-4, 2003.

Šimůnek, J., van Genuchten, M. T.: Modeling nonequilibrium flow and transport processes using HYDRUS, Vadose Zone Journal 7 (2), 782–797, doi:10.2136/vzj2007.0074, 2008.

Sprenger, M., Tetzlaff, D., Buttle, J., Laudon, H., Soulsby, C.: Water ages in the critical zone of long-term experimental sites in northern latitudes, Hydrol. Earth Syst. Sci., 2018.

Uffink, G. J. M.: Analysis of dispersion by the random walk method, PhD thesis, Delft University of Technology, 1990.

Uhlenbrook, S.: Catchment hydrology – a science in which all processes are preferential, Hydrol. Process., 20, 3581–3585, https://doi.org/10.1002/hyp.6564, 2006.

van Dam, J. C., Groenendijk, P., Hendriks, R. F. A., Kroes, J. G.: Advances of modeling water flow in variably saturated soils with SWAP, Vadose Zone Journal 7 (2), 640–653, doi:10.2136/vzj2007.0060, 2008.

van der Velde, Y., Heidbüchel, I., Lyon, S. W., Nyberg, L., Rodhe, A., Bishop, K., Troch, P. A.: Consequences of mixing assumptions for time-variable travel time distributions, Hydrological Processes: An International Journal 29 (16), 3460–3474, https://doi.org/10.1002/hyp.10372, 2015.

van Schaik, L., Palm, J., Klaus, J., Zehe, E., and Schröder, B.: Linking spatial earthworm distribution to macropore numbers and hydrological effectiveness, Ecohydrology, 7, 401–408, https://doi.org/10.1002/eco.1358, 2014.

Weiler, M.: An infiltration model based on flow variability in macropores: development, sensitivity analysis and applications, J. Hydrol., 310, 294–315, https://doi.org/10.1016/j.jhydrol.2005.01.010, 2005.

Weiler, M.: Mechanisms controlling macropore flow during infiltration. Dye tracer experiments and simulations, PhD thesis, ETHZürich, Zürich, 2001.

Whitmer, S., Baker, L., Wass, R.: Loss of bromide in a wetland tracer experiment, Journal of environmental quality 29 (6), 2043–2045, doi:10.2134/jeq2000.00472425002900060043x, 2000.

Workman, SR., Skaggs, R. W.: PREFLO. A water management model capable of simulating preferential flow. Transactions of the ASAE 33 (6), 1939–1948, doi: 10.13031/2013.31562, 1990.

Wrb, I. W.G.: World reference base for soil resources 2014, update 2015, International soil classification system for naming soils and creating legends for soil maps. World Soil Resources Reports 106, 2015

Zehe, E.: Stofftransport in der ungesättigten Bodenzone auf verschiedenen Skalen, PhD thesis, Mitteilungen des Instituts für Wasserwirtschaft und Kulturtechnik der Universität Karlsruhe (TH), Karlsruhe, 1999.

Zehe, E.; Flühler, H.: Slope scale variation of flow patterns in soil profiles, J. Hydrol., 247 (1-2), 116–132, https://doi.org/10.1016/S0022-1694(01)00371-7, 2001a.

Zehe, E.; Flühler, H.: Preferential transport of isoproturon at a plot scale and a field scale tile-drained site, J. Hydrol. 247 (1-2), 100–115, https://doi.org/10.1016/S0022-1694(01)00370-5, 2001b.

Zehe, E., Blöschl, G.: Predictability of hydrologic response at the plot and catchment scales. Role of initial conditions, Water Resour. Res., 40 (10), https://doi.org/10.1029/2003WR002869, 2004.

Zehe, E. and Jackisch, C.: A Lagrangian model for soil water dynamics during rainfall-driven conditions, Hydrol. Earth Syst. Sci., 20, 3511–3526, https://doi.org/10.5194/hess-20-3511-2016, 2016.

Zehe, E., Maurer, T., Ihringer, J., and Plate, E.: Modeling water flow and mass transport in a loess catchment, Phys. Chem Earth Pt. B,,26, 487–507, https://doi.org/10.1016/S1464-1909(01)00041-7, 2001.
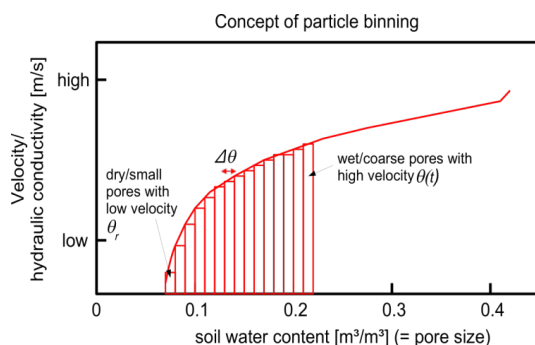
Figure 1. Concept of particle binning. All particles within a grid element are subdivided into bins (= red rectangles) of different pore sizes. Dependent on their related bin the particles travel at different flow velocities.
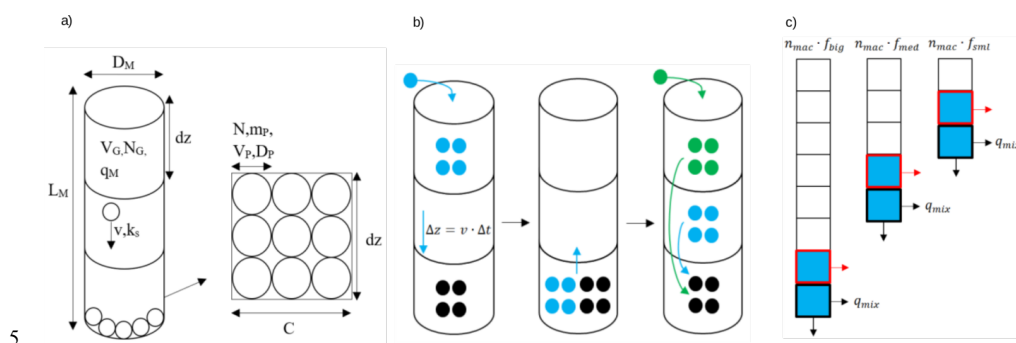
Figure 2. Conceptual visualization of a) structure of a macropore and concept of cubic storage, b) particle displacement and macropore filling as well as c) macropore depth distribution and diffusive mixing from macropores into matrix. With D_M, L_M, $dz(\Delta z)$ as the diameter, length of a macropore and the length of a grid element and where k_s is the saturated hydraulic conductivity of a macropore, v the advective velocity of a particle, V_G the volume of a grid element, N_G the total number of water particles fitting into a grid element, q_M the flux density of a macropore, m_P the mass of a particle, V_P the volume of a particle, D_P the diameter of a particle, N the total possible amount of particles having contact to the lateral surface of a grid element, C the circumference of a grid element, Δt the simulation time step, $nmac$ the total number of macropores, f the distribution factors and q_{mix} the macropore-matrix mixing fluxes.

Table 1. Simulation and tracer experiment parameters as well as soil hydraulic parameters after Schäfer (1999) at the sites 23, 31 and Spechtacker. Where k_s is the saturated hydraulic conductivity of the matrix, θ_s the saturated soil water content, θ_r the residual soil water content, α the inverse of an air entry value, n a quantity characterizing pore size distribution, s the storage coefficient and ρ_b the bulk density.

Parameter	Site 23	Site 31	Spechtacker
Irrigation duration [hh:mm]	02:10	02:10	02:30
Irrigation intensity [mm/h]	10.36	10.91	11.1
Br-concentration of irrigation water [kg/m³]	0.165	0.165	0.165
Recovery rate [%]	77	76	95
Soil moisture in 15 cm [%]	20.5	25.3	27.4
Soil moisture in 30 cm [%]	25.3	15.9	-
Soil moisture in 45 cm [%]	28.1	13	-
Soil moisture in 60 cm [%]	29.6	13.4	-
Simulation time [s]		86400 (=1 Day)	
Time step [s]		120	
Particle number in matrix [-]	1 Mill.	1 Mill.	2 Mill.
Particle number in pfd [-]	-	-	10 k
Soil type	Calcaric Regosol	Calcaric Regosol	Colluvic Regosol
k_s [m/s]	$0.50 \cdot 10^{-7}$	$0.50 \cdot 10^{-6}$	$2.50 \cdot 10^{-6}$
θ_s	0.44	0.44	0.4
θ_r	0.06	0.06	0.04
α [1/m]	0.4	0.4	1.9
n [-]	2.06	2.06	1.25
s [-]	0.26	0.45	0.38
ρ_b [kg/m³]	1300	1300	1500
nmac [-]	-	-	16
dmac [m]	-	-	0.005
Length of grid element dz_{pfd} [m]	-	-	0.05
mac. big[m]	-	-	1
mac. med[m]	-	-	0.8
mac. sml[m]	-	-	0.5
f big [-]	-	-	0.13
f mid [-]	-	-	0.19
f sml [-]	-	-	0.68

Table 2. Parameter ranges of the sensitivity analyses and configurations of macropore depth distribution and distribution factors (c.f. Figure 9).

Parameter	Value range			
k_s [m/s]	10^{-6} - 10^{-5} (step: $1\cdot10^{-6}$)			
$dmac$ [m]	$0.035 - 0.08$ (step: 0.005)			
$nmac$ [-]	$11 - 20$ (step: 1)			
mac. depth distr. config.	**1**	**2**	**3**	
mac. big [m]	-1	-0.8	-0.6	
mac. med [m]	-0.8	-0.6	-0.4	
mac. sml [m]	-0.6	-0.4	-0.2	
distr. factors config.	**1**	**2**	**3**	**4**
f big [-]	0.13	0.3	0	0.5
f med [-]	0.19	0.3	0.2	0.3
f sml [-]	0.68	0.3	0.8	0.2
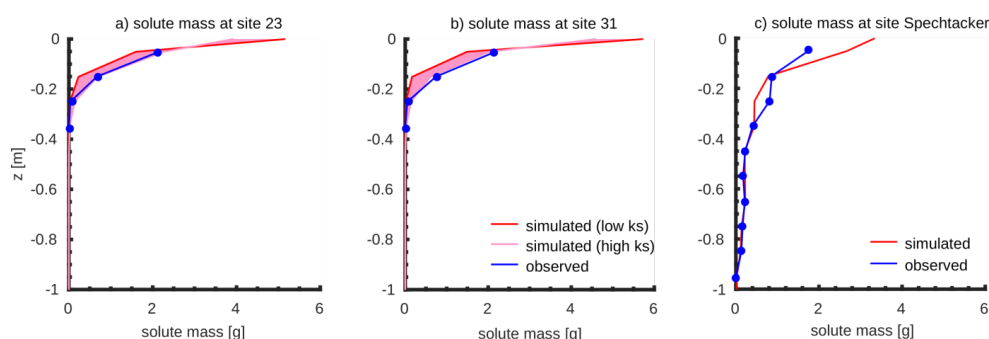
Figure 3. Comparison of final simulated and observed mass profiles of the matrix at the two well-mixed sites 23 + 31 (a+b) and at the preferential flow site Spechtacker (c). The rose area shows the range of the simulated profiles with different model parameter setups.
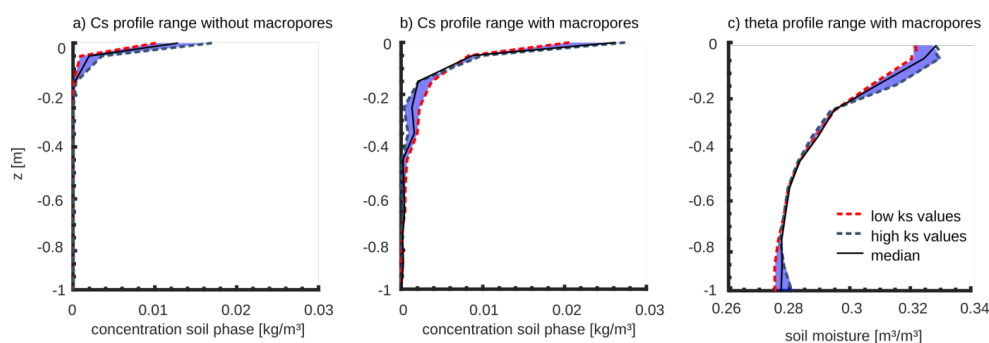
Figure 4. Final simulated concentration (Cs) profiles and soil moisture (*theta*) profiles of the soil matrix a) without and b+c) with macropores at different k_s values. The blue area shows the possible range of simulated profiles with different k_s values.
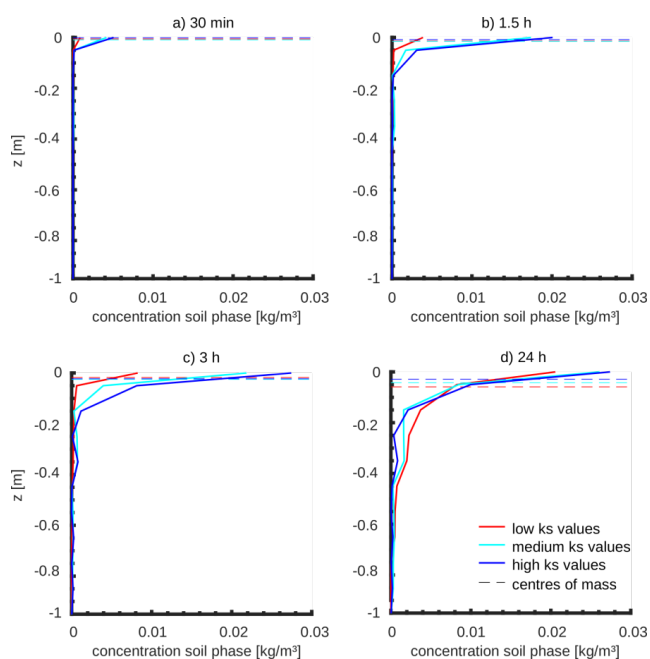
Figure 5. Time series of solute concentration profiles and centres of mass at different k_s values during the rainfall event (a+b), shortly after it (c) and at the end of simulation (d).
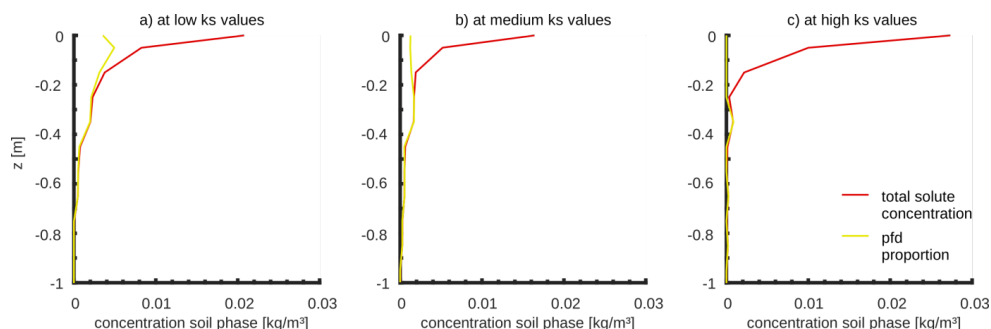
Figure 6. Final concentration profiles at a) low, b) medium and c) high k_s values and the proportion of solutes which originates from the macropores.
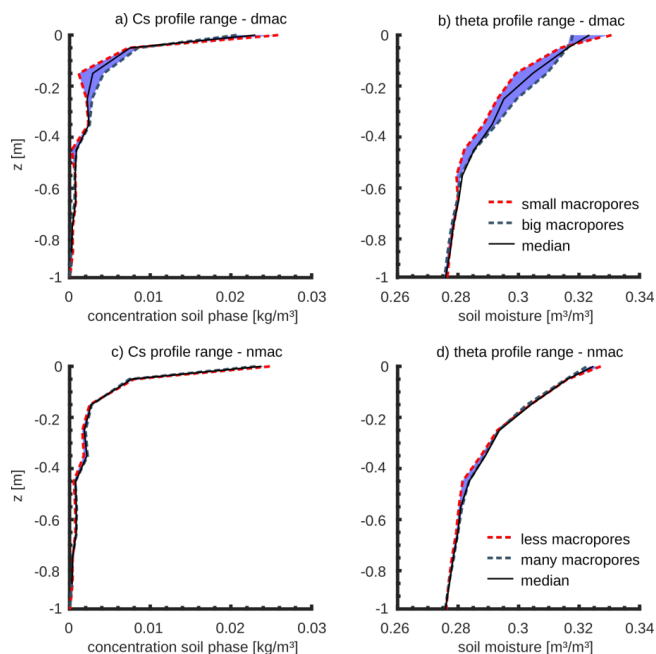
Figure 7. Final simulated concentration (*Cs*) profiles and soil moisture (*theta*) profiles of the soil matrix at different macropore diameters (*dmac*) (a+b) and macropore numbers (*nmac*) (c+d).
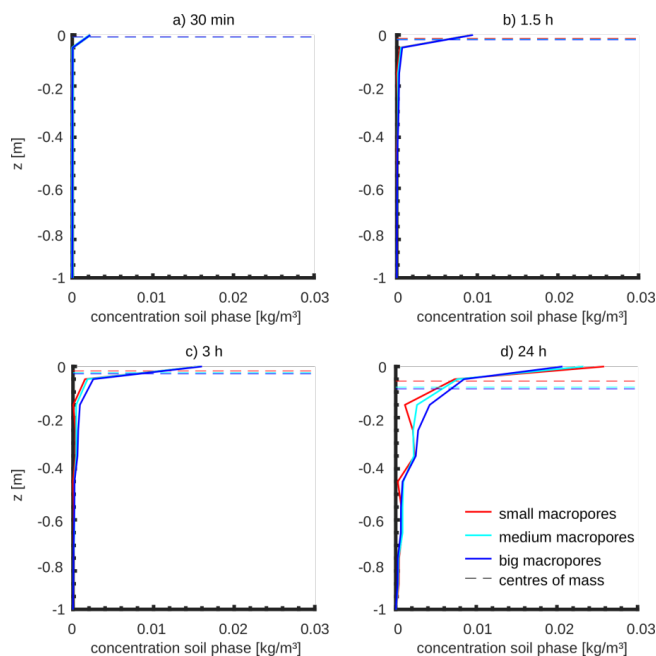
Figure 8. Time series of solute concentration profiles and centres of mass at different macropore diameters (*dmac*) during the rainfall event (a+b), shortly after it (c) and at the end of simulation (d).
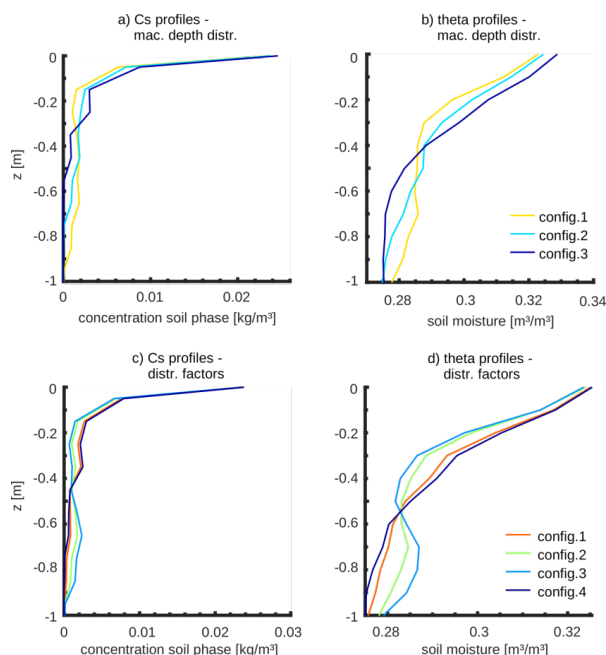
Figure 9. Final simulated concentration (*Cs*) profiles and soil moisture (*theta*) profiles of the soil matrix at three different macropore depth distribution configurations (a+b) and at four different distribution factor configurations (c+d) (c.f. Table 2).